Supporting Information - New Journal of Chemistry

Synthesis, structure and thermolysis of oxazagermines and oxazasilines

*Felix Dannenberg,[a] Günther Thiele,[b,c] Eike Dornsiepen,[b] Stefanie Dehnen,[b] Michael Mehring[a,]**

[a] *Technische Universität Chemnitz, Fakultät für Naturwissenschaften, Institut für Chemie, Professur Koordinationschemie, 09107 Chemnitz, Germany*

[b] *Fachbereich Chemie and Wissenschaftliches Zentrum für Materialwissenschaften, Philipps-Universität Marburg, Hans-Meerwein-Straße 4, 35043 Marburg, Germany*

[c] *present address: University of California, Department of Chemistry, Berkeley, California 94720, United States*

Molecular structures of compounds **1**, **2**, **3**, **5**, **6** and **8** (R_a enantiomer) and crystal data collection and refinement information

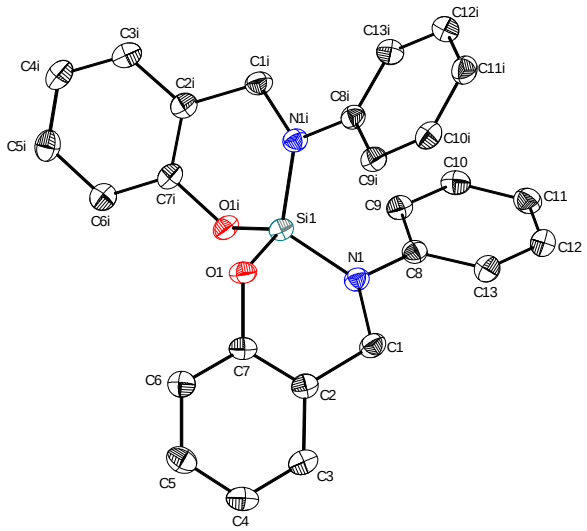

Figure S 1 Molecular structure of **1** in the solid state (50% probability level of displacement ellipsoids, hydrogen atoms are omitted for clarity). Selected bond lengths [Å] and bond angles [°]: Si1-O1 1.6396(9), Si1-N1 1.7033(10), O1-Si1-O1i 110.04(7), O1-Si1-N1 104.31(4), O1-Si1-N1i 111.01(4), N1-Si1-N1i 116.21(7). Symmetry transformations used to generate equivalent atoms: i denotes -x, y, 1.5-z.

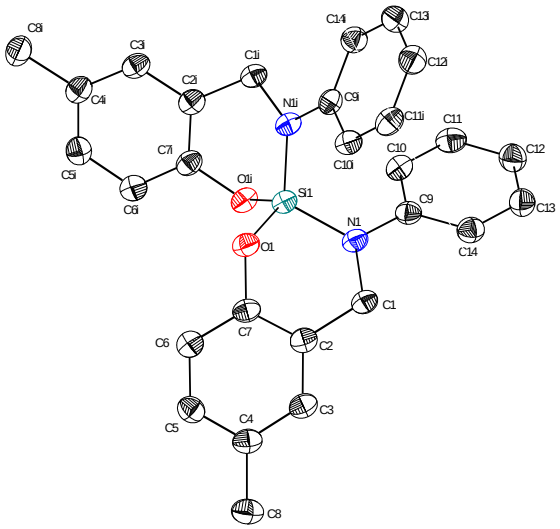

Figure S 2 Molecular structure of **2** in the solid state (50% probability level of displacement ellipsoids, hydrogen atoms are omitted for clarity). Selected bond lengths [Å] and bond angles [°]: Si1-O1 1.6434(13), Si1-N1 1.7055(15), O1-Si1-O1i 109.59(9), O1-Si1-N1 104.32(7), O1-Si1-N1i 110.90(7), N1-Si1-N1i 116.82(10). Symmetry transformations used to generate equivalent atoms: i denotes 1-x, 1-y, z.

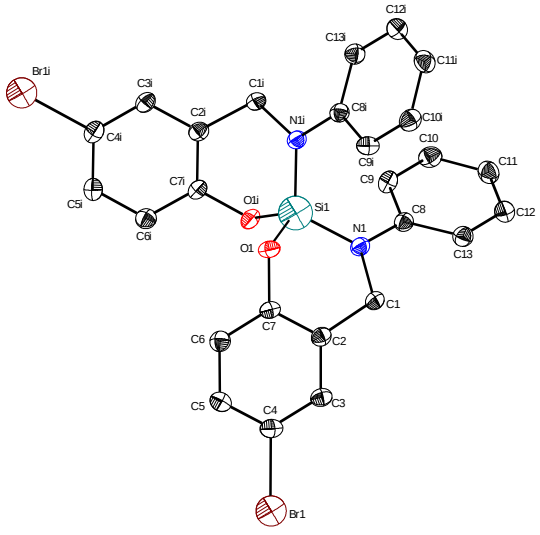

Figure S 3 Molecular structure of **3** in the solid state (50% probability level of displacement ellipsoids, hydrogen atoms are omitted for clarity). Selected bond lengths [Å] and bond angles [°]: Si1-O1 1.641(2), Si1-N1 1.705(2), C4-Br1 1.902(3), O1-Si1-O1i 109.00(17), O1-Si1-N1 103.88(11), O1-Si1-N1i 111.12(10), N1-Si1-N1i 117.77(19). Symmetry transformations used to generate equivalent atoms: i denotes 1-x, 1-y, z.

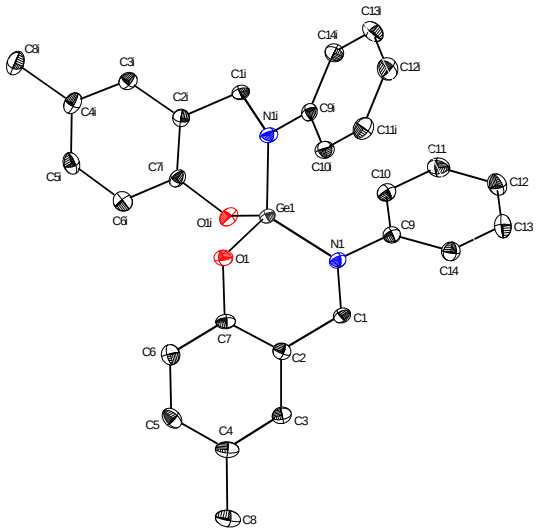

Figure S 4 Molecular structure of **5** in the solid state (50% probability level of displacement ellipsoids, hydrogen atoms are omitted for clarity). Selected bond lengths [Å] and bond angles [°]: Ge1-O1 1.7743(12), Ge1-N1 1.8035(15), O1-Ge1-O1i 109.55(9), O1-Ge1-N1 102.74(6), O1-Ge1-N1i 110.30(6), N1-Ge1-N1i 121.06(10). Symmetry transformations used to generate equivalent atoms: i denotes 2-x, -y, z.

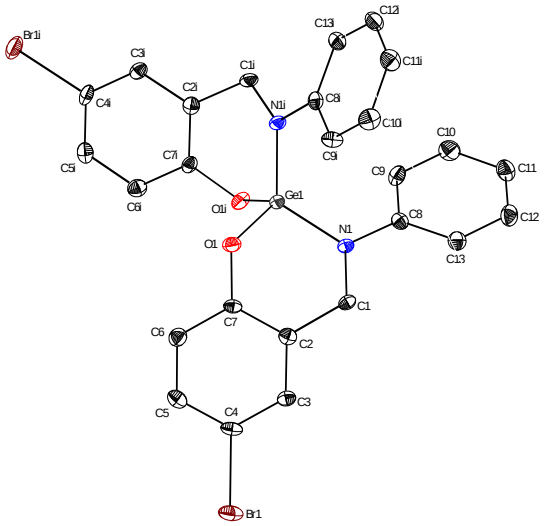

Figure S 5 Molecular structure of **6** in the solid state (50% probability level of displacement ellipsoids, hydrogen atoms are omitted for clarity). Selected bond lengths [Å] and bond angles [°]: Ge1-O1 1.7752(17), Ge1-N1 1.801(2), O1-Ge1-O1i 108.36(12), O1-Ge1-N1 102.21(8), O1-Ge1-N1i 111.02(8), N1-Ge1-N1i 121.68(14). Symmetry transformations used to generate equivalent atoms: i denotes 2-x, 2-y, z.

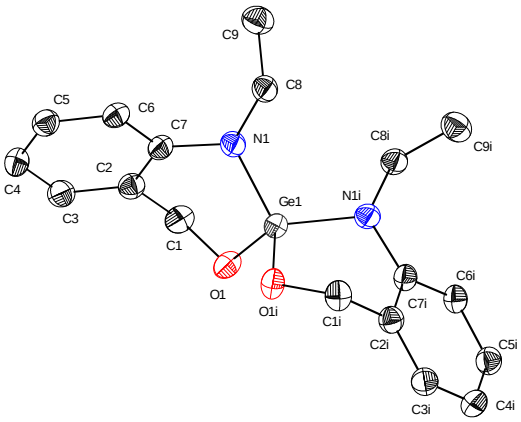

Figure S 6 Molecular Structure of **8** (R_a enantiomer) in the solid state (50% probability level of displacement ellipsoids, hydrogen atoms are omitted for clarity). Selected bond lengths [Å] and bond angles [°]: Ge1-O1 1.760(2), Ge1-N1 1.809(2), O1-Ge1-O1i 105.09(13), O1-Ge1-N1 102.51(9), O1-Ge1-N1i 117.48(9), N1-Ge1-N1i 112.23(15). Symmetry transformations used to generate equivalent atoms: i denotes 1-x, y, -z.

Table S 1 Compilation of crystal data collection and refinement information

parameters	**1**	**2**	**3**	**4**	**5**	**6**	**7**	**8** (S_a)	**8** (R_a)	**9**
emperical formula	$C_{26}H_{22}N_2O_2Si$	$C_{28}H_{26}N_2O_2Si$	$C_{26}H_{20}Br_2N_2O_2Si$	$C_{26}H_{22}N_2O_2Ge$	$C_{28}H_{26}N_2O_2Ge$	$C_{26}H_{20}Br_2N_2O_2Ge$	$C_{20}H_{26}N_2O_2Ge$	$C_{18}H_{22}N_2O_2Ge$	$C_{18}H_{22}N_2O_2Ge$	$C_{13}H_{11}NOGe$
formula weight	422.54	450.60	580.35	467.05	495.10	624.85	399.02	370.96	370.97	539.63
temperature / K	100	100	100	100	100	100	100	100	100	100
wavelength / Å	0.71073	0.71073	0.71073	0.71073	0.71073	0.71073	0.71073	0.71073	0.71073	0.71073
crystal system	orthorhombic	orthorhombic	orthorhombic	orthorhombic	orthorhombic	orthorhombic	monoclinic	monoclinic	monoclinic	triclinic
space group	*Pbcn*	*Fdd*2	*Fdd*2	*Pbcn*	*Fdd*2	*Fdd*2	$P2_1/c$	*C*121	*C*2	*P*-1
unit cell dimensions	*a* = 14.8114(6)	*a* = 15.2934(11)	*a* = 14.9435(6)	*a* = 14.8477(10)	*a* = 15.2579(8)	*a* = 14.9416(7)	*a* = 9.0089(2)	*a* = 12.1559(11)	*a* = 12.1426(11)	*a* = 6.8500(3)
	b = 8.5394(4)	*b* = 32.451(3)	*b* = 32.8797(14)	*b* = 8.5189(4)	*b* = 32.8165(17)	*b* = 33.2294(19)	*b* = 10.1226(2)	*b* = 7.3998(6)	*b* = 7.4037(5)	*b* = 6.8808(3)
	c = 16.8172(9)	*c* = 9.2736(6)	*c* = 9.4404(3)	*c* = 17.0779(8)	*c* = 9.2818(5)	*c* = 9.4680(7)	*c* = 20.3118(7)	*c* = 9.3532(7)	*c* = 9.3422(8)	*c* = 23.2208(9)
	α = 90°	*α* = 90°	*α* = 90°	*α* = 90°	*α* = 90°	*α* = 90°	*α* = 90°	*α* = 90°	*α* = 90°	*α* = 90.720(3)°
	β = 90°	*β* = 90°	*β* = 90°	*β* = 90°	*β* = 90°	*β* = 90°	*β* = 92.923(2)°	*β* = 103.252(6)°	*β* = 103.205(7)°	*β* = 90.263(3)°
	γ = 90°	*γ* = 90°	*γ* = 90°	*γ* = 90°	*γ* = 90°	*γ* = 90°	*γ* = 90°	*γ* = 90°	*γ* = 90°	*γ* = 104.661(3)°
volume, Z	2127.05(17) Å^3, 4	4602.4(6) Å^3, 8	4638.4(3) Å^3, 8	2160.1(2) Å^3, 4	4647.5(4) Å^3, 8	4700.9(5) Å^3, 8	1849.89(8) Å^3, 4	818.93(12) Å^3, 2	817.66(12) Å^3, 2	1058.72(8) Å^3, 2
density (calc.)	1.319 g·cm^{-3}	1.301 g·cm^{-3}	1.662 g·cm^{-3}	1.436 g·cm^{-3}	1.415 g·cm^{-3}	1.766 g·cm^{-3}	1.433 g·cm^{-3}	1.504 g·cm^{-3}	1.507 g·cm^{-3}	1.693 g·cm^{-3}
absorption coefficient	0.137 mm^{-1}	0.131 mm^{-1}	3.575 mm^{-1}	1.444 mm^{-1}	1.347 mm^{-1}	4.730 mm^{-1}	1.672 mm^{-1}	1.882 mm^{-1}	1.885 mm^{-1}	2.867 mm^{-1}
F (000)	888	1904	2320	960	2048	2464	832	384	384	544
crystal size / mm^3	0.15 x 0.13 x 0.10	0.15 x 0.13 x 0.12	0.15 x 0.13 x 0.11	0.17 x 0.15 x 0.11	0.44 x 0.41 x 0.30	1.00 x 0.78 x 0.41	0.21 x 0.19 x 0.08	0.51 x 0.33 x 0.19	0.30 x 0.20 x 0.10	0.21 x 0.17 x 0.12
θ range	2.422 to 26.716°	2.511 to 26.688°	2.478 to 26.693°	2.39 to 26.73°	2.48 to 30.62°	2.45 to 30.24°	2.008 to 29.193°	3.247 to 26.711°	2.24 to 26.74°	2.632 to 29.162°
limiting indices	-18 ≤ h ≤ 16	-19 ≤ h ≤ 19	-18 ≤ h ≤ 18	-18 ≤ h ≤ 18	-18 ≤ h ≤ 21	-21 ≤ h ≤ 15	-12 ≤ h ≤ 12	-15 ≤ h ≤ 15	-15 ≤ h ≤ 15	-9 ≤ h ≤ 9
	-10 ≤ k ≤ 10	-40 ≤ k ≤ 40	-41 ≤ k ≤ 41	-10 ≤ k ≤ 10	-34 ≤ k ≤ 45	-46 ≤ k ≤ 45	-13 ≤ k ≤ 13	-9 ≤ k ≤ 9	-9 ≤ k ≤ 8	-9 ≤ k ≤ 9
	-21 ≤ l ≤ 21	-11 ≤ l ≤ 11	-11 ≤ l ≤ 11	-21 ≤ l ≤ 21	-13 ≤ l ≤ 12	-13 ≤ l ≤ 11	-27 ≤ l ≤ 27	-11 ≤ l ≤ 11	-11 ≤ l ≤ 11	-31 ≤ l ≤ 31
reflections collected	20817	12368	26568	23252	10682	11322	52127	4713	5407	47679
independent reflections	2253	2440	2450	2296	3209	3223	4955	1717	1684	5680
R_{int}	0.0792	0.0475	0.0567	0.0981	0.0312	0.0355	0.0473	0.1085	0.0840	0.0370
completeness to θ	0.997	1.00	1.00	1.00	0.89	0.91	0.989	1.00	0.98	0.992
Absorption correction T_{min} / T_{max}	0.9420 / 0.9850	0.850 / 0.988	0.437 / 0.732	0.7601 / 0.8504	0.6275 / 0.7461	0.4574 / 0.7460	0.4943 / 0.7688	0.403 / 0.747	0.6085 / 0.7970	0.4331 / 0.7745
data/restraints/parameters	2022/0/185	2268/1/151	2435/1/150	1557/0/185	3040/1/151	3007/1/150	4774/0/230	1700/1/106	1678/1/106	5257/0/289
S	1.061	0.977	1.076	0.902	1.104	1.056	1.094	1.065	1.095	1.081
final *R* indices [I > 2σ (*I*)]	R_1 = 0.0367,	R_1 = 0.0256,	R_1 = 0.0224,	R_1 = 0.0271,	R_1 = 0.0272,	R_1 = 0.0277,	R_1 = 0.0268,	R_1 = 0.0398,	R_1 = 0.0277,	R_1 = 0.0251,
	wR_2 = 0.0887	wR_2 = 0.0602	wR_2 = 0.0559	wR_2 = 0.0530	wR_2 = 0.0582	wR_2 = 0.0532	wR_2 = 0.0684	wR_2 = 0.0958	wR_2 = 0.0707	wR_2 = 0.0601
R indices (all data)	R_1 = 0.0424,	R_1 = 0.0287,	R_1 = 0.0229,	R_1 = 0.0642,	R_1 = 0.0306,	R_1 = 0.0321,	R_1 = 0.0287,	R_1 = 0.0405,	R_1 = 0.0277	R_1 = 0.0301,
	wR_2 = 0.0927	wR_2 = 0.0608	wR_2 = 0.0563	wR_2 = 0.0609	wR_2 = 0.0596	wR_2 = 0.0545	wR_2 = 0.0697	wR_2 = 0.0962	wR_2 = 0.0707	wR_2 = 0.0618
max./min. residual electron density	0.267 / -0.399 e Å^3	0.199 / -0.168 e Å^3	0.208 / -0.572 e Å^3	0.328 / -0.245 e Å^3	0.269 / -0.695 e Å^3	0.317 / -0.508 e Å^3	0.384 / -0.471 e Å^3	0.427 / -1.118 e Å^3	0.594 / -0.263 e Å^3	0.432 / -0.501 e Å^3
absolute structure parameter[1]		-0.02(5)	-0.015(5)		0.034(8)	0.023(8)		-0.024(16)	-0.002(12)	

ATR-FTIR spectroscopy

a)

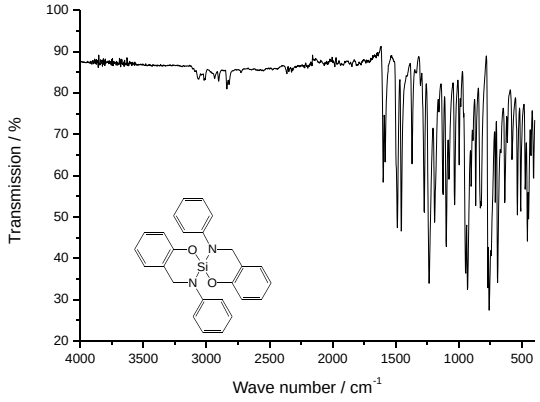

b)

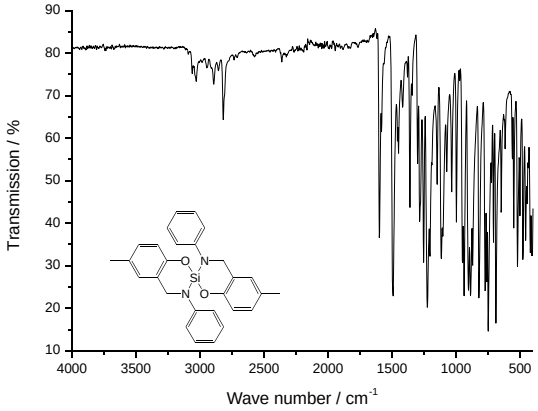

c)

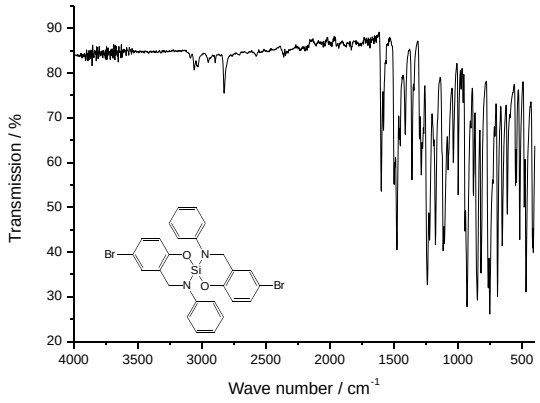

d)

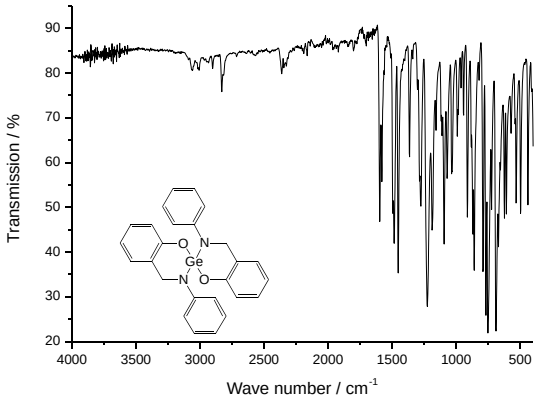

e)

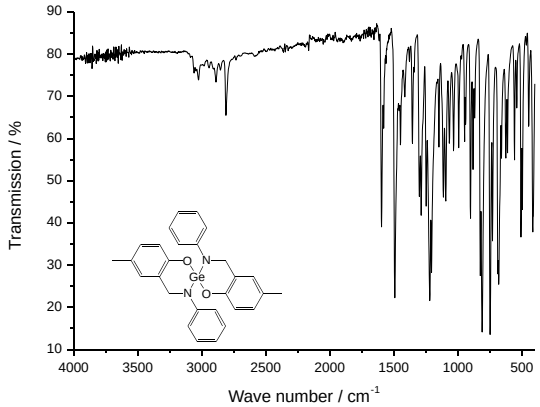

f)

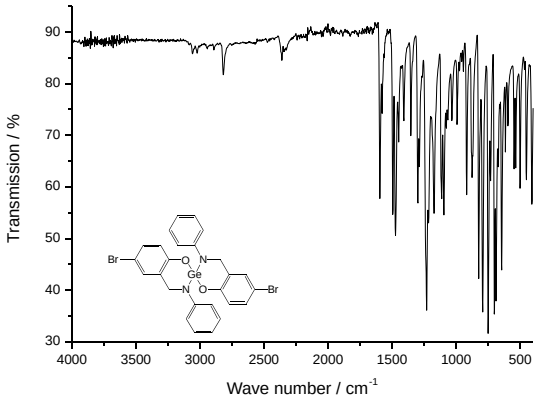

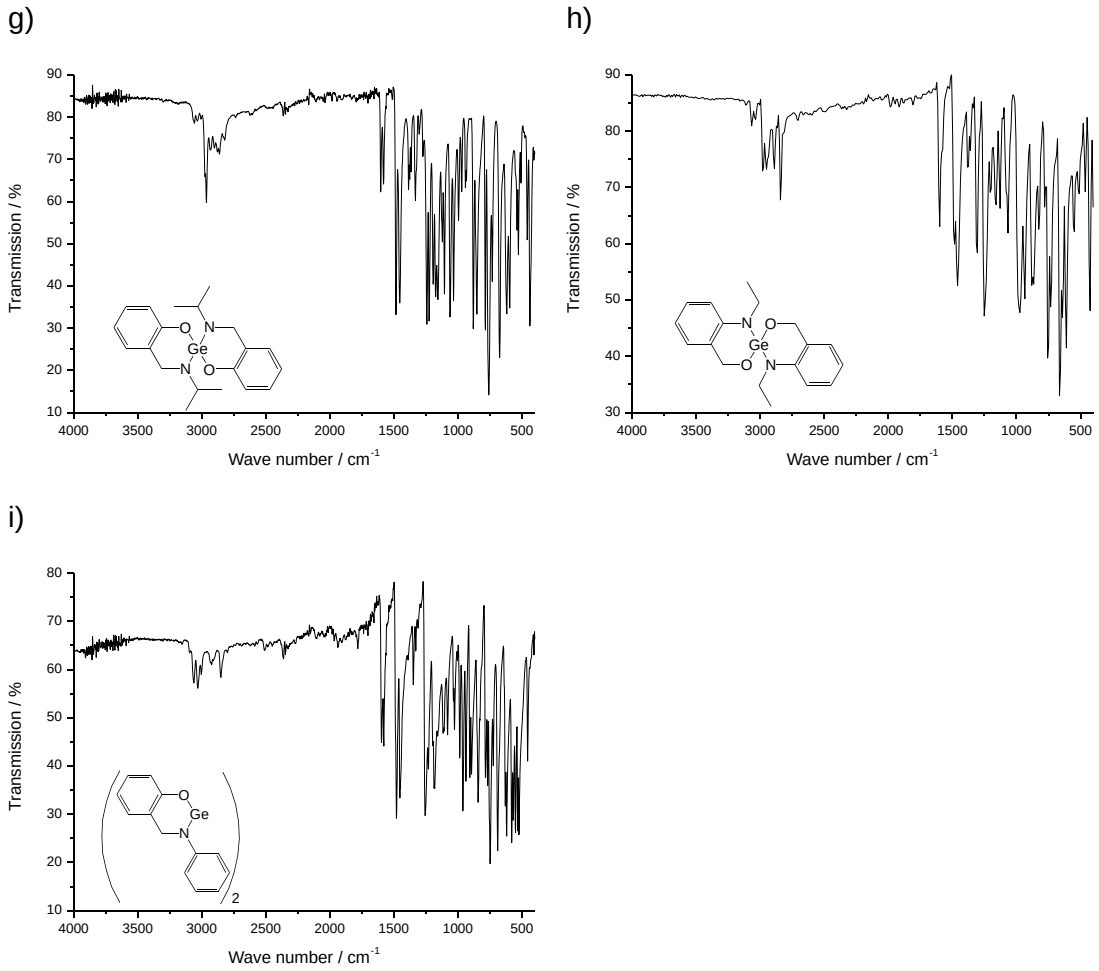

Figure S 7 ATR-FTIR spectra of compounds a) **1**, b) **2**, c) **3**, d) **4**, e) **5**, f) **6** g) **7** h) **8** i) **9**.

NMR Spectra of compound **9**

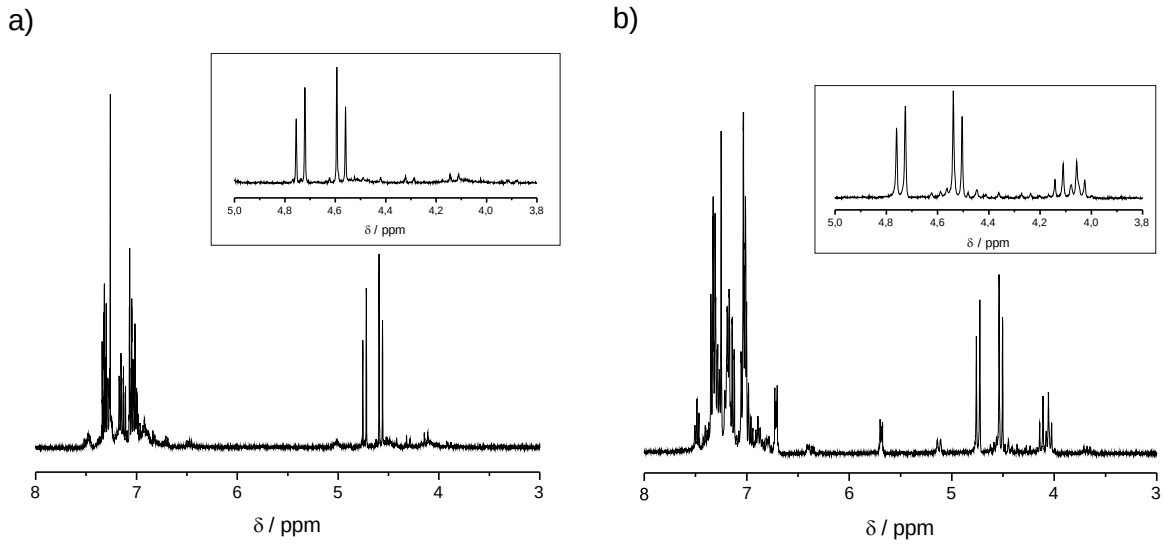

Figure S 8 NMR spectra of compound **9** 24 h after dissolution in $CDCl_3$. a) NMR spectrum recorded at ambient temperature and b) NMR spectrum recorded at -50°C.

TGA-analysis

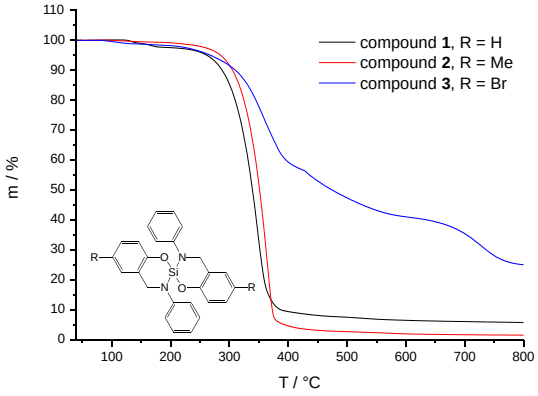

Figure S 9 Thermogravimetric analysis of silicon compounds **1** (black line), **2** (red line), **3** (blue line); heating rate 10 K · min^{-1}, N_2 atmosphere, N_2 volume flow of 20 ml · min^{-1}.

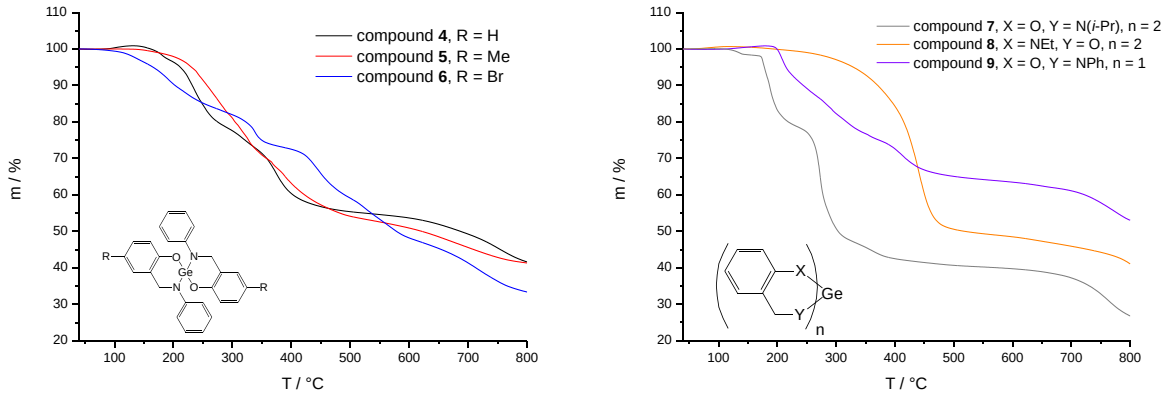

Figure S 10 Thermogravimetric analysis of germanium compounds **4** (black line), **5** (red line), **6** (blue line) are depicted in the left picture and compound **7** (grey line), **8** (orange line) and **9** (violet line) in the right picture; heating rate 10 K · min^{-1}, N_2 atmosphere, N_2 volume flow of 20 ml · min^{-1}. Please note, that the masses of the compounds **4**, **8** and **9** increase slightly at the beginning, which might be attributed to the presence of oxygen or moisture within the nitrogen gas.

PXRD pattern of carbonized germanium compounds **4** – **9** for different peak temperatures

a)

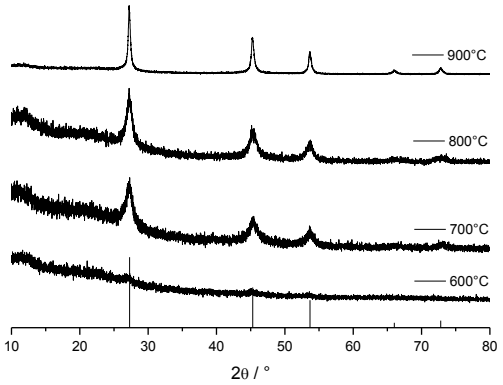

precursor

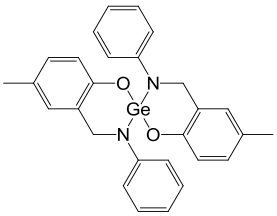

b)

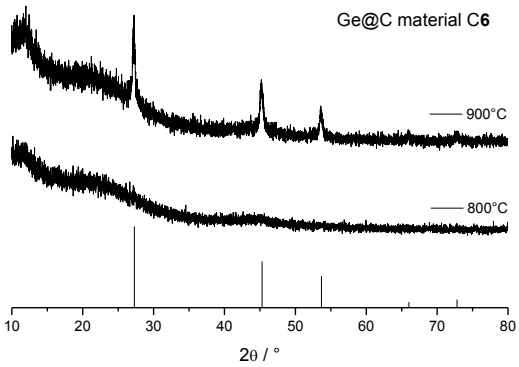

precursor

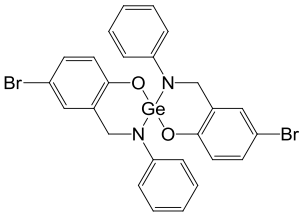

c)

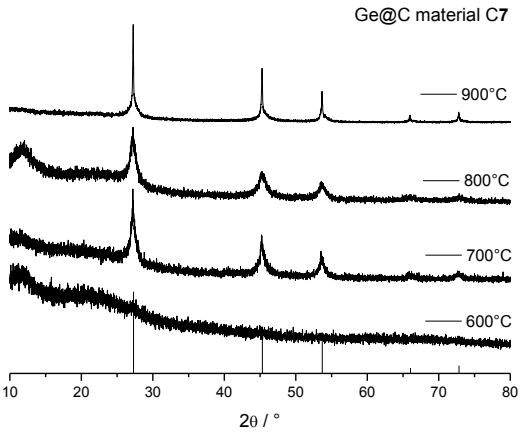

precursor

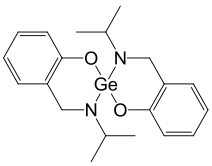

d)

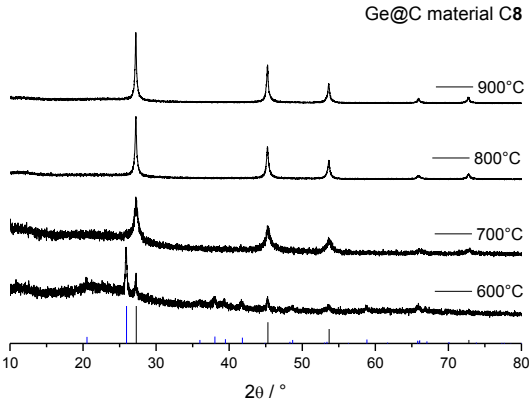

precursor

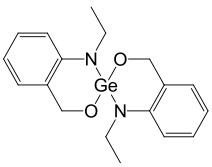

e)

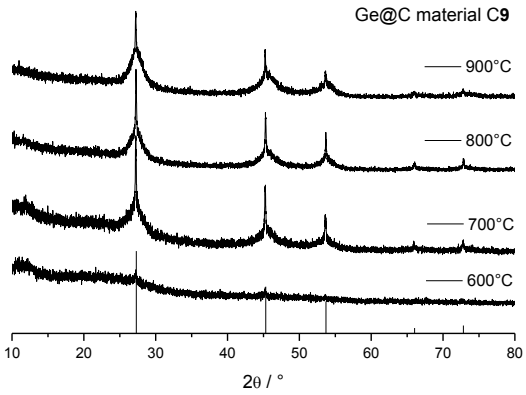

precursor

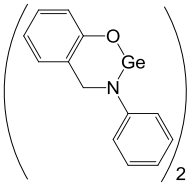

Figure S 11 Temperature-dependent formation of crystalline germanium after carbonization of a) compound **5** b) compound **6** c) compound **7** d) compound **8** e) compound **9** in the temperature range 600°C - 900°C or 800°C - 900°C with bars for standard diffraction pattern of cubic germanium (ICDD no. 00-004-0545, black bars) and hexagonal germanium dioxide (ICDD no. 00-036-1463, blue bars).

Elemental composition of selected Ge@C materials

*Material C**4***

Table S 2 CHN-analysis of material C**4** and the resulting carbon, hydrogen and nitrogen contents

Temperature	residue	C / % CHN-analysis	H / % CHN-analysis	N / % CHN-analysis
600 °C	39 %	56.28	1.75	2.43
700 °C	38 %	58.29	0.92	2.61
800 °C	37 %	56.28	0.81	1.94
900 °C	38 %	59.85	0.25	1.79

*Material C**9***

Table S 3 CHN-analysis of material C**9** and the resulting carbon, hydrogen and nitrogen contents

Temperature	residue	C / % CHN-analysis	H / % CHN-analysis	N / % CHN-analysis
600 °C	49 %	45.38	1.34	1.55
700 °C	39 %	47.56	0.43	1.80
800 °C	44 %	45.12	0.31	1.40
900 °C	40 %	46.75	0.03	1.05

Selected SEM Pictures for materials C**4**, C**8** and C**9**

*Material C**4***

a) b) c)

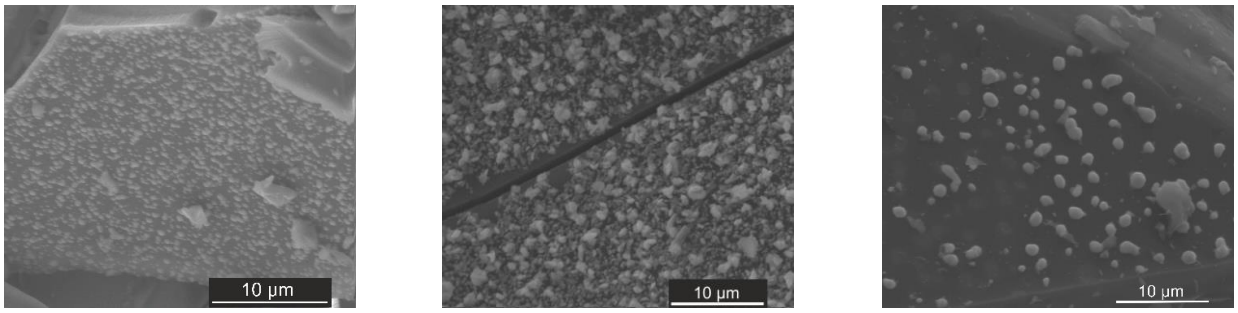

600°C 800°C 900°C

Figure S 12 SEM pictures with 10 µm scale bar for materials a) C**4**_600, b) C**4**_800 and c) C**4**_900.

*Material C**9***

a) b) c)

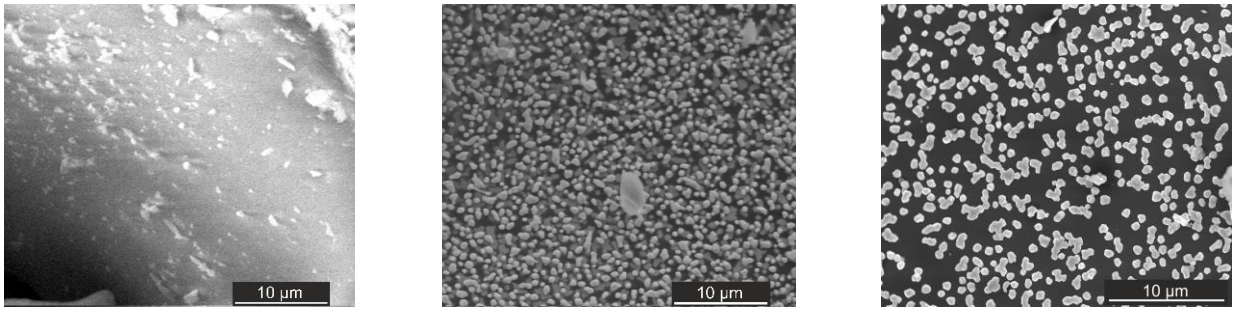

600°C 800°C 900°C

d)

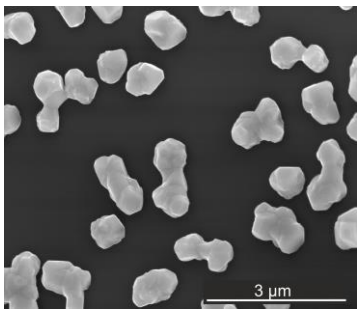

900°C

Figure S 13 SEM pictures with 10 µm scale bar for materials a) C**9**_600, b) C**9**_800, c) C**9**_900 and enlarged view with 3 µm scale bar for materials d) C**9**_900.

N_2-sorption measurements

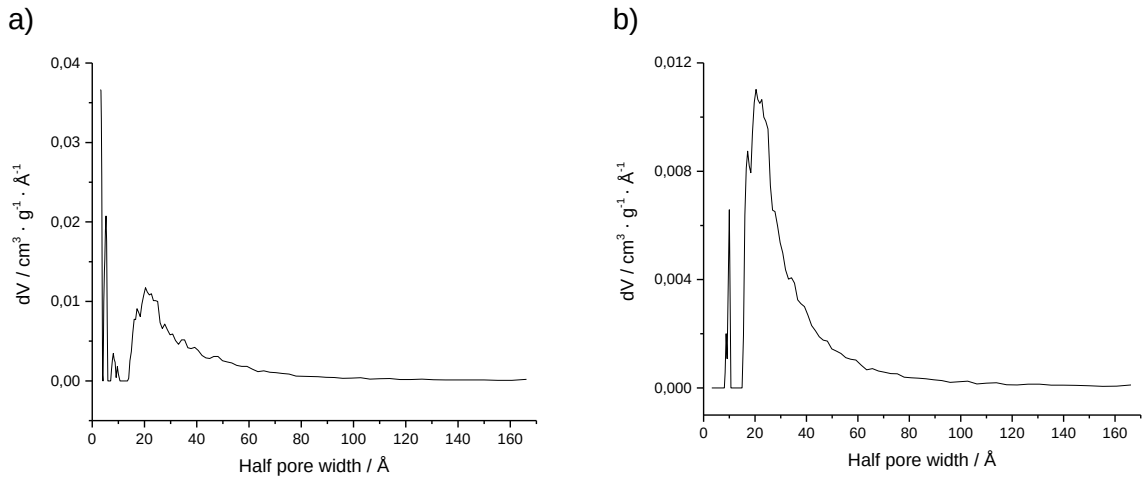

Figure S 14 Pore size distribution of a) C**4**_900 and b) C**9**_900. The pore size distributions were determined according to the QSDFT model for slit and cylindrical pores using the adsorption branch for carbon materials.

References – Supporting Information

[1] H. D. Flack, *Acta Crystallogr., Sect. A* **1983**, *39*, 876.